ELECTROMAGNETIC MODELING OF OBJECTIVE LENSES IN COMBINATION WITH INTEGRATED LENS ANTENNAS

Maarten J.M. van der Vorst, Peter J.I.de Maagt* and Matti H.A.J. Herben
Eindhoven University of Technology, Faculty of Electrical Engineering P.O. Box 513,
5600 MB Eindhoven, The Netherlands, e-mail: M.J.M.v.d.Vorst@ele.tue.nl
*European Space Agency ESTEC, P.O. Box 299, 2200 AG Noordwijk, The Netherlands

Abstract—**In this paper the electromagnetic modeling of an integrated (eye) lens antenna with an additional objective lens is decribed. Two different field calculation methods, Geometrical/Physical Optics (GO-PO) and Physical/ Physical Optics (PO-PO), are compared for various diameter over wavelength ratios of the integrated lens antenna. The main difference between both methods is that in case of PO-PO, the entire eye-lens contributes to the PO currents at a point on the outer objective lens surface, while only one GO ray contributes in case of the GO-PO method. The comparisons show that the GO-PO method can be used as a good first-order approximation. However, if a more accurate prediction of the beam pattern is required, then the PO-PO method should be applied.**

I. Introduction

IT IS OBVIOUS that with the availability of integrated planar antenna technology extremely compact receivers can be made. This technology is quite suitable for imaging arrays which are of great interest for both space astronomy and atmospheric research. Particularly in astronomy most of the spectral line emitting regions are usually spatially extended over many observing beams in the sky and therefore mapping is required to understand the astrophysics of these regions. In atmospheric research, imaging is used for profiling, rain sounding, etc.

For imaging purposes the hyperhemispherical integrated lens antenna (HILA) is often applied in combination with an objective lens, because of the nearly aberration free performance. Another reason for using an objective/integrated lens antenna combination is the matching of the beam of the HILA to the beam required to properly feed a typical Cassegrain or Gregorian telescope.

Usually, the objective lens is placed in the Fresnel zone of the integrated lens antenna and this does not validate the use of the far-field radiation pattern of the HILA in the analysis of the combined quasi-optical system. Then, the most straightforward way of modeling the objective/integrated lens antenna combination is by means of Geometrical Optics (GO) from the planar feed of the HILA to the outer objective lens surface and subsequently Physical Optics (PO) to obtain the far-field pattern. However, the GO analysis does not include the wave diffraction due to the limited lens size of the HILA. To improve the accuracy of the modeling, a PO method will be described which takes the radiation from the entire eye-lens surface into account to calculate the PO currents on the outer surface of the objective lens. A Fourier decomposition is applied to the second PO integral to speed up the calculations.

II. Design

A. General Aspects

For certain applications, like imaging and quasi-optical beam transformers, it is needed to include an objective lens in front of the integrated lens antenna, and the resulting configuration is shown in Fig. 1. Here the objective lens is placed in the Fresnel zone of the lens antenna which is generally the case.

When the objective lens is used as a beam transformer, the incoming Gaussian beam (first order) is changed into another Gaussian beam with a different beam waist or phase center. For imaging it is important that a sharp image of a certain object is obtained and this means that an incoming plane wave has to be focused to the planar feed of the lens antenna. In the next section it will be shown that a number of different objective lenses can be applied for this purpose.

B. Lens Types

For imaging applications the shape of the objective lens is designed as to produce a spherical or nearly spherical phase front at the eye-lens aperture. To achieve this two different surface-lens types can be used [1]:

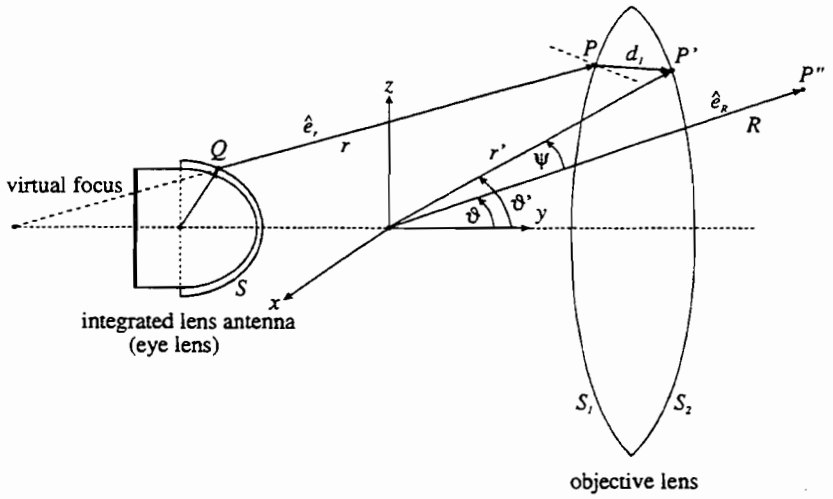

Fig. 1. *Geometry of integrated lens antenna (with matching layer) in combination with an objective lens.*

- single-surface lenses
  - hyperbolic inner and flat outer surface
  - spherical inner and flat outer surface
  - meniscus lens
- dual-surface lenses
  - flat inner and curved outer surface
  - curved inner and outer surface

For the single-surface lenses refraction of the incident wave only takes place at one surface of the objective lens, while for the dual-surface lenses both surfaces change the direction of propagation.

For imaging applications it is required that the side lobes of the quasi-optical system are low and this cannot be achieved by means of a flat field distribution in the aperture. The meniscus lens will give a nearly uniform field distribution and therefore this lens type is not preferred. A disadvantage of the dual-surface lenses is that their fabrication is somewhat more elaborate than that of the single-surface ones. In practice the spherical lens is more often used than the hyperbolic one, and therefore in this paper emphasis will be put on the spherical single-surface lens. This means that in, Fig. 1, surface S_1 is part of a sphere and S_2 is flat. It is noted that the spherical single-surface lens does not transform an incoming plane wave into a spherical one, but in the thin lens approximation (thickness of lens negligible to focal distance) it does.

III. Electromagnetic Modeling

A. PO-PO

When the objective lens is placed in the Fresnel region of the integrated lens antenna, the far-field approximations can not be used and it becomes necessary to start with the original Physical Optics integrals. Silver [2] showed that for the electric and magnetic fields in any observation point P the following equations hold:

$$\underline{E}(P) = \frac{-j}{4\pi\omega\varepsilon_0}\iint_S \Big[(\underline{J}_s\cdot\nabla)\nabla + k^2\underline{J}_s + j\omega\varepsilon_0(\underline{M}_s\times\nabla)\Big]\frac{e^{-jkr}}{r}dS \quad (1)$$

$$\underline{H}(P) = \frac{-j}{4\pi\omega\mu_0}\iint_S \Big[(\underline{M}_s\cdot\nabla)\nabla + k^2\underline{M}_s - j\omega\mu_0(\underline{J}_s\times\nabla)\Big]\frac{e^{-jkr}}{r}dS \quad (2)$$

In the integrands of these equations, the operator ∇ acts on the source element coordinates and therefore the following results are valid [2]:

$$\nabla\Big(\frac{e^{-jkr}}{r}\Big) = \Big(jk+\frac{1}{r}\Big)\frac{e^{-jkr}}{r}\hat{e}_r \quad (3)$$

and

$$(\underline{J}_s\cdot\nabla)\nabla\Big(\frac{e^{-jkr}}{r}\Big) = \Big[-k^2(\underline{J}_s\cdot\hat{e}_r)\hat{e}_r + \frac{3}{r}\Big(jk+\frac{1}{r}\Big)\hat{e}_r(\underline{J}_s\cdot\hat{e}_r) - \frac{\underline{J}_s}{r}\Big(jk+\frac{1}{r}\Big)\Big]\frac{e^{-jkr}}{r} \quad (4)$$

If the fields are evaluated in the Fresnel and Fraunhofer region of the integrated lens antenna ($r > 0.62\sqrt{D^3/\lambda}$), the terms with $1/r$ and $1/r^2$ can be

neglected and the fields of (1) and (2) become:

$$\underline{E}(P) = \frac{-jk^2}{4\pi\omega\varepsilon_0}\iint_S \Big[\underline{J}_s - (\underline{J}_s \cdot \hat{e}_r)\hat{e}_r + \frac{1}{Z_0}(\underline{M}_s \times \hat{e}_r)\Big]\frac{e^{-jkr}}{r}dS \quad (5)$$

$$\underline{H}(P) = \frac{-jk^2}{4\pi\omega\mu_0}\iint_S \Big[\underline{M}_s - (\underline{M}_s \cdot \hat{e}_r)\hat{e}_r - Z_0(\underline{J}_s \times \hat{e}_r)\Big]\frac{e^{-jkr}}{r}dS \quad (6)$$

These equations show that the fields in point P can be treated as an infinite summation of spherical waves (spherical wave expansion) originating from the lens antenna surface. The complex excitation of these waves is given by the equivalent electric ($\underline{J}_s$) and magnetic ($\underline{M}_s$) current densities, which can be calculated from the pattern of the planar feed in the dielectric lens by using:

$$\begin{aligned} \underline{J}_s &= \hat{n} \times \underline{H}(Q) \\ \underline{M}_s &= -\hat{n} \times \underline{E}(Q) \end{aligned} \quad (7)$$

Because the H-field of each individual spherical wave is related to the E-field according to:

$$\underline{H} = \frac{\hat{e}_r \times \underline{E}}{Z_0} \quad (8)$$

only the E-field will be considered in the remainder of this analysis. If the objective lens is included in the design, the refracted wave in point P on the inner surface propagates to point P' on the outer surface. To describe the fields and currents at the outer side of the lens, the influence of the lens has to be modeled. By means of Geometrical Optics each spherical wave can be traced through the lens, which means inclusion of the transmission coefficients, the spreading factor from the inner to the outer surface and an additional phase change. Finally, if all effects are accounted for, the following integral is obtained:

$$\underline{E}(P') = \frac{-jk^2}{4\pi\omega\varepsilon_0}\iint_S \Big[\underline{J}_s - (\underline{J}_s \cdot \hat{e}_r)\hat{e}_r + \frac{1}{Z_0}(\underline{M}_s \times \hat{e}_r)\Big]\overline{\overline{T}}_1\overline{\overline{T}}_2 D_F \frac{e^{-jkr-jk_d d_1}}{r}dS \quad (9)$$

with D_F the divergence factor, $\overline{\overline{T}}_1$ and $\overline{\overline{T}}_2$ the dyadic Fresnel transmission coefficients at S_1 and S_2 respectively, and d_1 the length of a ray inside the objective lens.

To obtain the far-field radiation pattern of the objective/integrated lens antenna combination, the Physical Optics equivalent current densities have to be computed at the outer objective lens surface and then the standard PO integrals can be determined.

B. GO-PO

In the previous section the PO-PO method was described, where the entire eye-lens surface is taken into account in the calculation of the fields in P'. Another method, which is extensively used in optics, is GO-PO and here only one ray from the planar feed to P' is used. This means that GO is applied from the feed to the outer surface of the objective lens. The validity of this method depends on the size of the eye lens, the distance between eye and objective lens and the frequency. The larger the eye lens is in terms of a wavelength, the more accurate the method will be.

Because the transmitted ray passes through two refraction points from feed to objective lens, the ray-tracing is more complex for this method than for the PO-PO method. In this paper hyperhemispherical eye lenses will be used, which offer the possibility of tracing the rays from the virtual focus to the objective lens (see Fig. 1). It should be noted that when this method is applied, the small lateral shift of the ray due to the matching layer will be neglected in the ray-tracing procedure [3].

C. Ray-tracing Procedure

In Sections III.A and III.B the electromagnetic fields were described on the outer objective lens surface (S_2). For an efficient PO integration scheme the equivalent currents, corresponding to these fields, must be defined in a regular grid. Of course this requires a ray-tracing procedure to find, for each grid point on S_2, the refraction points on the first lens surface (S_1) that correspond to the source points on the integrated lens antenna (see Fig. 1). In Fig. 2 the configuration for the ray-tracing and the symbols used are depicted.

First a center of the curved inner surface of the objective lens is defined (point C). For the spherical lens this corresponds to the real center of surface S_1. The cross-section plane that is shown in Fig. 2 contains the incident ray, the refracted ray and the normal vector in B, because the normal vector equals the unity vector from C to B. It contains also the vectors from C to P' and from C to Q. It should be clear that the wanted refraction

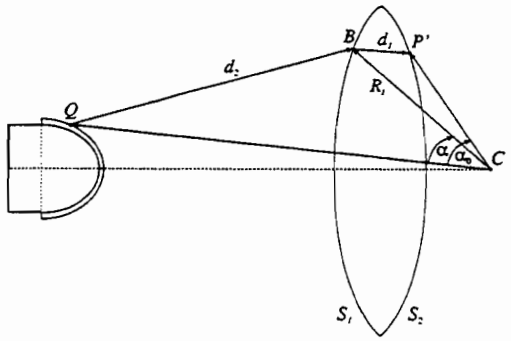

Fig. 2. *Ray-tracing from source point Q to grid point P' on second objective lens surface.*

point is to be found in this plane. The phase from source point to observation point is determined by the distances d_1 and d_2 which are given by:

$$d_1 = \sqrt{(CP')^2 + {R_l}^2 - 2(CP')R_l \cos(\alpha_0 - \alpha)} \tag{10}$$

$$d_2 = \sqrt{(CQ)^2 + {R_l}^2 - 2(CQ)R_l \cos\alpha} \tag{11}$$

with (CQ) and (CP') the distances from C to Q and from C to P', respectively. Refraction point B is found for an angle α, that corresponds to a minimum of the function $n_d d_1 + d_2$ (shortest electrical path length).

D. Far-field and Fourier Decomposition

Now that the fields at the second objective lens surface (S_2) are known, it is possible to compute the far-field of the total system (eye plus objective lens). For this PO is used and Eqs. (5) and (6) describe the fields in any observation point. However, because in this paper we are only interested in the far-field of the antenna system, a few approximations can be made [2] and these result in:

$$\underline{E}(P'') = \frac{-j\omega\mu_0 e^{-jkR}}{4\pi R} \iint_{S_2} \Big[\underline{J}'_s - (\underline{J}'_s \cdot \hat{e}_R)\hat{e}_R + \frac{1}{Z_0}(\underline{M}'_s \times \hat{e}_R)\Big] e^{jk r' \cos\psi} dS_2 \tag{12}$$

with $\underline{J}'_s$ and $\underline{M}'_s$ the equivalent current densities on the second objective lens surface (S_2). Every far-field pattern, beam and Gaussian beam efficiency calculation requires many of these double-integral computations to be performed, which are very time-consuming. Therefore, it would be elegant to rewrite (simplify) Eq. (12) and speed up the calculations. By using a similar expansion as mentioned in Ref. [4], Eq. (12) is rewritten as:

$$\underline{E}(P'') = c_1 \iint_{S_2} \underline{N}(x', z') e^{jk r' \cos\psi} dS_2 \tag{13}$$

with c_1 and $\underline{N}(x', z')$ defined as:

$$c_1 = \frac{-j\omega\mu_0 e^{-jkR}}{4\pi R} \tag{14}$$

$$\underline{N}(x', z') = \underline{J}'_s - (\underline{J}'_s \cdot \hat{e}_R)\hat{e}_R + \frac{\underline{M}'_s \times \hat{e}_R}{Z_0} \tag{15}$$

The next step is to transform the integration over the, generally curved, surface S_2 to an integration over a plane aperture with diameter D. To do so, the normal vector of S_2 is needed and the Cartesian coordinates (x',z') of point P' are transformed to polar coordinates (ρ',φ'). Then Eq. (13) changes to:

$$\underline{E}(P'') = \int_0^{2\pi} \int_0^{D/2} \underline{G}(\rho', \varphi') e^{jk r' \cos\psi} d\rho'\, d\varphi' \tag{16}$$

with

$$\underline{G}(\rho', \varphi') = \underline{N}(x', z') c_1 \rho' \sqrt{1 + \left(\frac{\partial S_2}{\partial x'}\right)^2 + \left(\frac{\partial S_2}{\partial z'}\right)^2} \tag{17}$$

To calculate $\underline{G}$ in (17), x' and z' have to be substituted by $\rho' \sin\varphi'$ and $\rho' \cos\varphi'$, respectively.

By describing P' and P'' with their spherical coordinates, $(r', \vartheta', \varphi')$ and (R, ϑ, φ), and inserting these into (16), the next equation is found:

$$\underline{E}(P'') = \int_0^{2\pi} \int_0^{D/2} e^{k r' \cos\vartheta \cos\vartheta'} \underline{G}(\rho', \varphi') e^{jk\rho' \sin\vartheta \cos(\varphi - \varphi')} d\rho'\, d\varphi' \tag{18}$$

In the following only one component (x) of the electric field will be considered, because the others can be treated similarly. A new variable is defined and directly decomposed into its Fourier series:

$$K(\rho', \varphi') = e^{k r' \cos\vartheta \cos\vartheta'} G_x(\rho', \varphi') = \sum_{m=-\infty}^{\infty} k_m(\rho') e^{jm\varphi'} \tag{19}$$

The coefficients k_m can be found simply by taken a Fast Fourier Transform (FFT) of the function K. By substituting the Fourier series of K into (18)

the following expression for the x-component of the electric field is obtained:

$$E_x(P'') = \int_0^{2\pi} \int_0^{D/2} \sum_{m=-\infty}^{\infty} k_m(\rho') e^{jm\varphi'} e^{jk\rho' \sin\vartheta \cos(\varphi-\varphi')} d\rho' \, d\varphi' \quad (20)$$

Interchanging the integration variables and using the known relation for the m^{th}-order Bessel function J_m [5]:

$$J_m(u) = \frac{1}{2\pi} \int_0^{2\pi} e^{j(u\sin\varphi' - m\varphi')} d\varphi' \quad (21)$$

gives:

$$E_x(P'') = 2\pi \int_0^{D/2} \sum_{m=-\infty}^{\infty} k_m(\rho') J_{-m}(k\rho' \sin\vartheta) d\rho' \quad (22)$$

if the observation point P'' is located in the plane $\varphi = \pi/2$. It should be mentioned that in the integral of Eq. (22) the original integration interval $[-\pi, \pi]$ is changed to $[0, 2\pi]$. Of course also other observation planes can be chosen, but then an extra phase term should be added:

$$E_x(P'') = 2\pi \int_0^{D/2} \sum_{m=-\infty}^{\infty} k_m(\rho') J_{-m}(k\rho' \sin\vartheta) e^{jm(\pi/2-\varphi)} d\rho' \quad (23)$$

In principal an infinite number of terms need to be included in the Fourier series decomposition. However, computer simulations showed that, dependending on the value of ρ', 11-15 Fourier terms are sufficient to describe the function K. However, to numerically evaluate Eq. (23) the integral from 0 to $D/2$ has to be written as a finite summation. In the software that is used to generate the results for this paper, the integral is carried out by applying Gaussian quadratures. Then only a small number, compared to conventional integration procedures, of fixed ρ' are needed.

The CPU-time saving by using this decomposition was tested for an integrated lens antenna without objective lens. It was found that the computation time can be decreased by more than 50% if the number of observation points is larger than 80. Of course the time saving will be less for the complete quasi-optical system, because the calculation of the PO-currents on the outer objective lens surface is more elaborate than the calculation of the PO currents on the eye lens. Nevertheless, usually not only the far-field patterns are computed but also the efficiencies and then the Fourier decomposition will result in a more efficient use of the CPU time.

IV. Simulation Results

In the examples in this section the two different methods will be compared for various operating frequencies. To test the accuracy of the GO-PO method, the co- and cross-polar radiation patterns are computed and compared with the results from the more accurate PO-PO method. In Fig. 3 the patterns are depicted for an antenna system operating at 500, 1000 and 2000 GHz, where the diameter of the eye and objective lens are 6 and 30 mm, respectively. The hemispherical eye lens is made of silicon ($\varepsilon_r = 11.7$) and has an extension length of 0.877 mm (hyperhemispherical condition). To minimize the reflection losses, a quarter-wavelength matching layer is put on top of the silicon lens. For the 4.35 mm thick objective lens, with a spherical inner and flat outer surface, high densitiy polyethylene ($\varepsilon_r = 2.3$) is used and this lens is placed at a distance of 36.7 mm from the center of the eye lens. The radius of curvature of the inner surface of the objective lens is taken 28 mm, which results in an optimized directivity of more than 41 dBi at 500 GHz. As planar radiator a double slot is chosen with a length of $0.28\lambda_0$ and a separation between the slots equal to $0.16\lambda_0$. This feed design results in a good rotationally symmetric pattern within the eye lens.

It can be seen from Fig. 3 that the results obtained by the GO-PO and the PO-PO methods become more alike, observing the main lobe and the first side lobes, for increasing frequencies. This is expected as GO is a high-frequency technique. For the lower frequencies however the discrepancies are significant and therefore it can be said that the use of the more elaborate PO-PO method is necessary if an accurate prediction of the far-field patterns is needed. Furthermore, it should be noted that GO-PO method can be very useful to get a first-order approximation of the beam pattern, because the computation time is negligible compared to the PO-PO method.

V. Conclusions

Quasi-optical systems, consisting of a feed with an additional objective lens, can play an important role in applications like imaging. The modeling of these systems becomes more complex due to this extra lens. In this paper two calculation methods are compared with each other, GO-PO and PO-PO, of which GO-PO is the more traditional and PO-PO the more accurate. The analysis showed that GO-PO can be used as a good first-order approximation of the main lobe and the first sidelobe. However, if a better prediction of the far-field pattern is required, then the field contribution of the entire eye-lens surface has to be included into the modeling and this is done by means of the PO-PO method.

Also in this paper, a time-efficient procedure is described for computing the far field of the entire quasi-optical system. The PO integrals are rewritten in such a way that a Fourier decomposition of the integrands can be made and this can decrease the computational effort by more than 50% if the far fields in many observation points are needed.

References

[1] A.D. Olver et al., *Microwave horns and feeds*, New York: IEEE Press, Ch. 11, 1994.

[2] S. Silver, *Microwave antenna theory and design*, McGraw-Hill, Ch. 3, 1949.

[3] M.J.M. van der Vorst, P.J.I. de Maagt and M.H.A.J. Herben, *Matching layers for integrated lens antennas*, Proceedings of the International Symposium on Antennas (JINA '96), pp. 511-515, 1996, Nice, France.

[4] V. Galindo-Israel and R. Mittra, *A new series representation for the radiation integral with application to reflector antennas*, IEEE Trans. Antennas and Propagat., vol. 25, pp. 631-641, 1977.

[5] F. Lösch, *Tables of higher functions*, Stuttgart: Teubner Verslagsgesellschaft, p. 145, 1966.

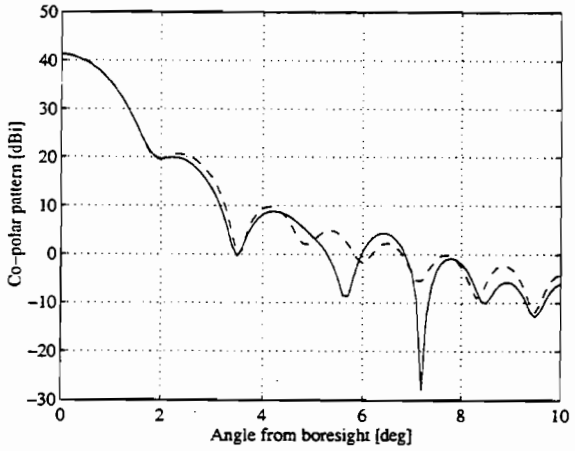

(a) $f = 500$ GHz

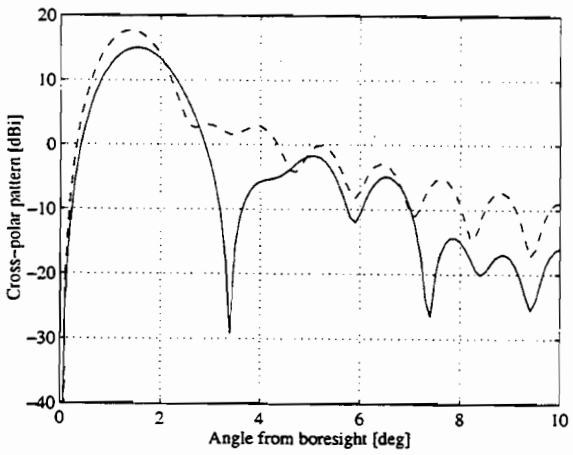

(b) $f = 500$ GHz

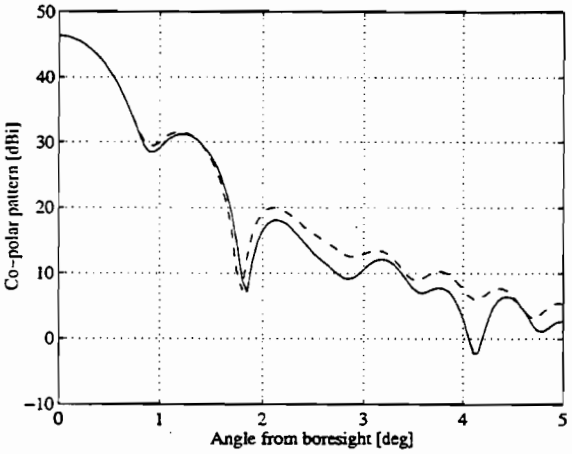

(c) $f = 1000$ GHz

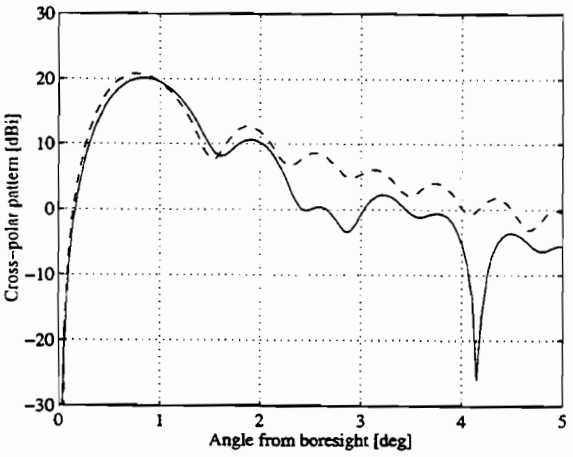

(d) $f = 1000$ GHz

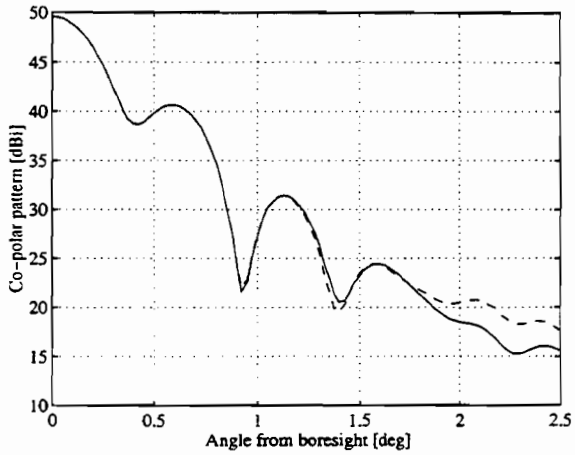

(e) $f = 2000$ GHz

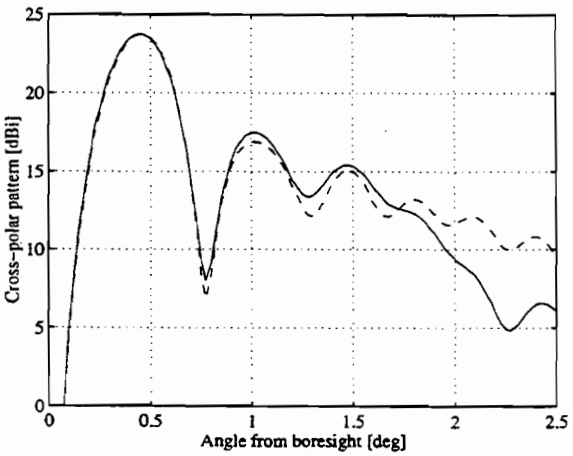

(f) $f = 2000$ GHz

Fig. 3. *Co- and cross-polar patterns for various frequencies (solid: PO-PO; dashed: GO-PO).*